Stem Cell Research 28 (2018) 29–32

Contents lists available at ScienceDirect

Stem Cell Research

journal homepage: www.elsevier.com/locate/scr

Lab Resource: Stem Cell Line

Generation of human embryonic stem cell line with heterozygous RB1 deletion by CRIPSR/Cas9 nickase

Jian Tu [a,b], Zijun Huo [a,c], Mo Liu [a], Donghui Wang [a], An Xu [a], Ruoji Zhou [a,d], Dandan Zhu [a], Julian Gingold [e], Jingnan Shen [b,**], Ruiying Zhao [a,**], Dung-Fang Lee [a,d,f,g,*]

[a] Department of Integrative Biology and Pharmacology, McGovern Medical School, The University of Texas Health Science Center at Houston, Houston, TX 77030, USA
[b] Department of Musculoskeletal Oncology, The First Affiliated Hospital of Sun Yat-sen University, Guangzhou 510080, China
[c] Department of Endocrinology, The First Affiliated Hospital of Sun Yat-sen University, Guangzhou 510080, China
[d] The University of Texas MD Anderson Cancer Center UTHealth Graduate School of Biomedical Sciences, Houston, TX 77030, USA
[e] Women's Health Institute, Cleveland Clinic Foundation, Cleveland, OH 44195, USA
[f] Center for Stem Cell and Regenerative Medicine, The Brown Foundation Institute of Molecular Medicine for the Prevention of Human Diseases, The University of Texas Health Science Center at Houston, Houston, TX 77030, USA
[g] Center for Precision Health, School of Biomedical Informatics and School of Public Health, The University of Texas Health Science Center at Houston, Houston, TX 77030, USA

ARTICLE INFO

Article history:
Received 8 November 2017
Received in revised form 7 January 2018
Accepted 18 January 2018
Available online 28 February 2018

ABSTRACT

The Retinoblastoma 1 (RB1) tumor suppressor, a member of the Retinoblastoma gene family, functions as a pocket protein for the functional binding of E2F transcription factors. About 1/3 of retinoblastoma patients harbor a germline *RB1* mutation or deletion, leading to the development of retinoblastoma. Here, we demonstrate generation of a heterozygous deletion of the *RB1* gene in the H1 human embryonic stem cell line using CRISPR/Cas9 nickase genome editing. The *RB1* heterozygous knockout H1 cell line shows a normal karyotype, maintains a pluripotent state, and is capable of differentiation to the three germline layers.

Resource table

Unique stem cell line identifier	CDMLe001-A
Alternative name(s) of stem cell line	H1-*RB1*(E16)$^{-/+}$
Institution	The University of Texas Health Science Center at Houston
Contact information of distributor	dung-fang.lee@uth.tmc.edu
Type of cell line	Human embryonic stem cell line
Origin	hESC line H1 (WA01) from WiCell Institute
Additional origin info	Sex: Male (46, XY)
Cell Source	Human blastocyst
Clonality	Clonal
Method of reprogramming	N/A
Genetic Modification	Yes
Type of Modification	Deletion of 50 bp in *RB1* exon 16.
Associated disease	Hereditary retinoblastoma
Gene/locus	13q14.1-14.2; *RB1* exon 16
Method of modification	CRISPR/Cas9 nickase
Name of transgene or resistance	None
Inducible/constitutive system	None
Date archived/stock date	11/7/2017
Cell line repository/bank	None
Ethical approval	Cell lines were used according to institutional guidelines. UTHealth approval number: SCRO-16-01

Resource utility

We generate a human embryonic stem cell (hESC) line with heterozygous *RB1* deletion to facilitate the modeling of the cancer etiology of hereditary retinoblastoma.

Resource details

Hereditary retinoblastoma patients commonly carry a heterozygous *RB1* mutation or deletion (Lin et al., 2017). Random sporadic damage to the remaining normal copy of RB1 in retinal cells initiates development of retinoblastoma. To provide a useful lab resource for scientists investigating hereditary retinoblastoma, we generated a heterozygous *RB1* deletion hESC line by targeting exon 16 of the *RB1* gene using the CRISPR/

* Correspondence to: D.-F. Lee, Department of Integrative Biology and Pharmacology, McGovern Medical School, The University of Texas Health Science Center at Houston, Houston, TX 77030, USA.
** Corresponding authors.
E-mail addresses: shenjingnan@126.com (J. Shen), ruiying.zhao@uth.tmc.edu (R. Zhao), dung-fang.lee@uth.tmc.edu (D.-F. Lee).

https://doi.org/10.1016/j.scr.2018.01.021
1873-5061/

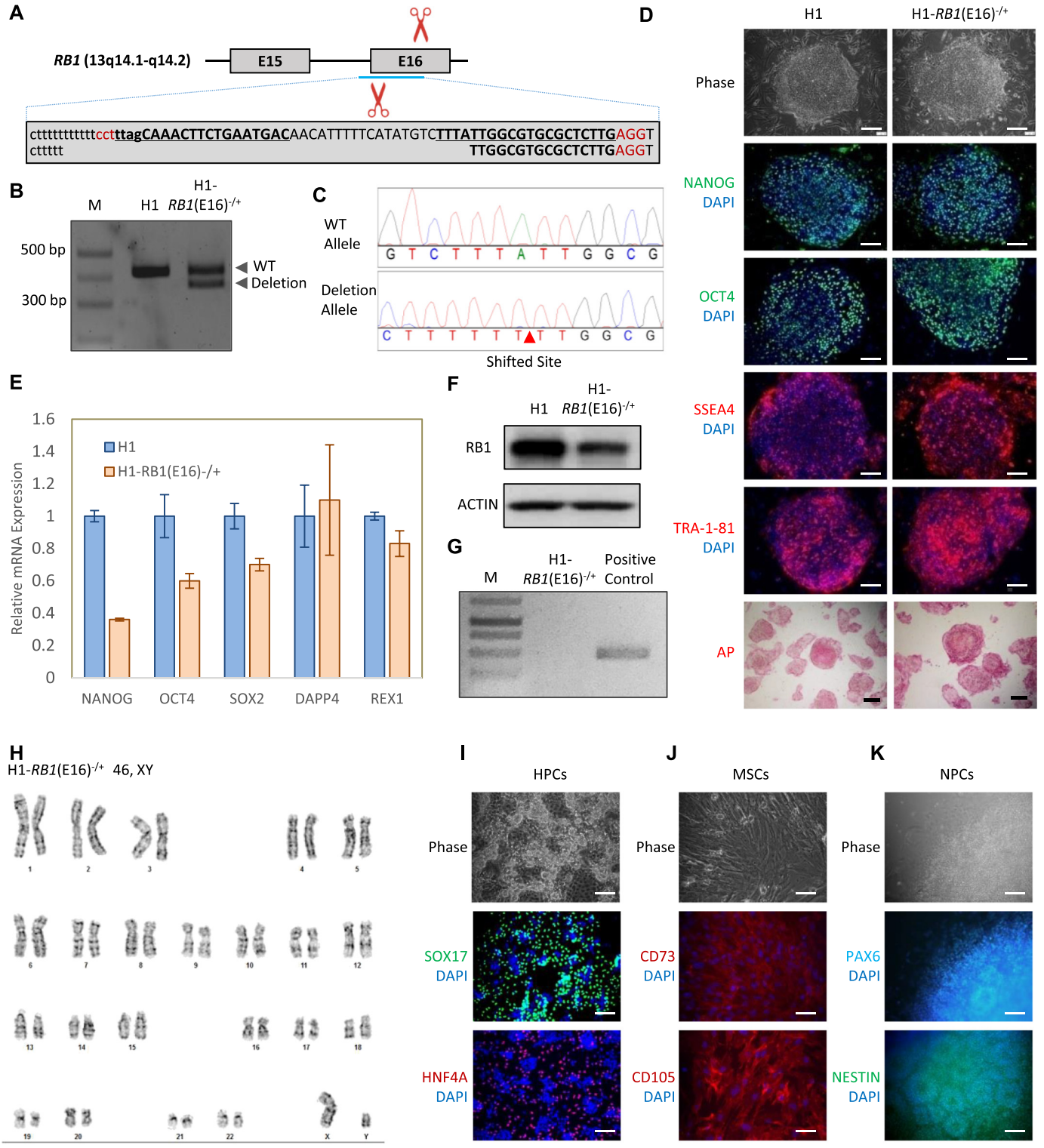

Fig. 1. Generation and characterization of the *RB1* heterozygous knockout hESC line H1-*RB1*(E16)$^{-/+}$. (A) Schematic overview of the gene targeting strategy to knockout *RB1* exon 16 using CRISPR/Cas9 nickase. *RB1* introns and exons are shown in lowercase and uppercase, respectively. The sgRNA target sites are underlined. (B) PCR confirms the deletion of the *RB1* exon 16 in the H1-*RB1*(E16)$^{-/+}$ line. (C) Sanger sequencing reveals the heterozygous deletion of the *RB1* exon16. (D) The H1-*RB1*(E16)$^{-/+}$ line expresses hESC pluripotency factors (NANOG and OCT4) and hESC surface markers (SSEA4 and TRA-1-81), and exhibits positive AP activity. Scale bar = 100 μm. (E) qRT-PCR reveals the expression of endogenous human NANOG, SOX2, OCT4, DPPA4, and REX1in H1-*RB1*(E16)$^{-/+}$ line. PCR reactions are normalized to GAPDH and plotted relative to expression levels in human H1 ESCs. Error bars indicate ± SEM of triplicates. (F) The H1-*RB1*(E16)$^{-/+}$ line presents the lower expression of RB1 protein. (G) The H1-*RB1*(E16)$^{-/+}$ line is mycoplasma-free. (H) The H1-*RB1*(E16)$^{-/+}$ line shows normal karyotype. (I-K) The H1-*RB1*(E16)$^{-/+}$ line maintains pluripotency. Immunofluorescence staining reveals that H1-*RB1*(E16)$^{-/+}$ line is capable of differentiating to endodermal (HPCs), mesodermal (MSCs) and ectodermal (NPCs) lineages. Scar bar = 100 μm.

Cas9 nickase gene editing system (Fig. 1A, the Cas9/sgRNA target sites are underlined and *RB1* introns and exons are presented in lowercase and uppercase, respectively).

hESC H1 cells were transfected with pX335-U6-Chimeric_BB-CBh-hSpCas9n(D10A) (Puro^{R}) plasmids carrying sgRNAs targeting exon 16 of the *RB1* gene. Electroporated cells were selected by puromycin. The

puromycin-resistant clones were picked up, isolated, and expanded. The *RB1* targeted regions were analyzed by PCR to demonstrate that only one allele was deleted (Fig. 1B). Primers surrounding exon 16 (amplifying both the wild-type and deleted alleles) were designed and the genetic region amplified by PCR and examined by Sanger sequencing. The mono-allelic 50-nucleotide-deletion was confirmed in the deleted allele, while the other allele retained its wild-type sequence (Fig. 1C). A premature stop codon was also noted in *RB1* exon 17 in the allele with a 50-nucleotide-deletion in one of two heterozygous *RB1* deletion hESC clones obtained and submitted for further characterization.

The H1-*RB1*(E16)$^{-/+}$ line maintains a classical tightly packaged dome-shape hESC morphology and expresses high levels of pluripotency transcription factors (NANOG and OCT4), hESC surface markers (SSEA4 and TRA-1-81) as well as alkaline phosphatase (AP) (Fig. 1D, scale bar 100 μm). The expression of pluripotency genes (*NANOG*, *OCT4*, *SOX2*, *DPPA4*, and *REX1*) in the H1-*RB1*(E16)$^{-/+}$ line was compared to the levels in parental H1 cells by quantitative real-time PCR. PCR reactions are normalized to *GAPDH*. The expression levels of all five pluripotency genes in the H1-*RB1*(E16)$^{-/+}$ line were comparable to those in parental H1 cells (Fig. 1E, error bars indicate ± SEM of triplicates). Immunoblotting results suggested that RB1 expression is lower in the H1-*RB1*(E16)$^{-/+}$ line than in parental H1 cells (Fig. 1F). PCR-based mycoplasma detection assay confirmed the cell line is mycoplasma-free (Fig. 1G). Karyotype analysis suggested that the H1-*RB1*(E16)$^{-/+}$ line does not contain any chromosomal abnormality (Fig. 1H). Additionally, the short tandem repeat (STR) profile of H1-*RB1*(E16)$^{-/+}$ cells was identical to that of their parental H1 cells (Supplementary Table S1). Furthermore, H1-*RB1*(E16)$^{-/+}$ cells maintained the potential to differentiate into all three germ layers as determined by their ability to differentiate to SOX17 and HNF4A-positive hepatic progenitor cells (HPCs, endodermal lineage) (Fig. 1I, scale bar 100 μm), CD73 and CD105-positive mesenchymal stem cells (MSCs, mesodermal lineage) (Fig. 1J, scale bar 100 μm) as well as PAX6 and NESTIN-positive neural progenitor cells (NPCs, ectodermal lineage) (Fig. 1K, scale bar 100 μm). In summary, the H1-*RB1*(E16)$^{-/+}$ line is pluripotent and demonstrates a normal karyotype. The H1-*RB1*(E16)$^{-/+}$ line provides a valuable cell resource to study the cancer etiology of hereditary retinoblastoma.

Materials and methods

Maintenance of hESCs

hESCs were maintained on Matrigel (Corning)-coated plates with StemMACS™ iPS-Brew XF (Miltenyi Biotec). StemMACS™ Passaging Solution XF (Miltenyi Biotec) was used to passage hESCs and Rock inhibitor (Calbiochem) was utilized to improve cell survival rate during replating.

Generation of RB1 heterozygous deletion hESC line by CRIPSR/Cas9 nickase gene editing methodology

A CRISPR guide targeting exon 16 of RB1 was designed using CRISPR Design website (http://crispr.mit.edu). Two sgRNAs (TTAGCAAACTTCTGAGTGAC and TTTATTGGCGTGCGCTCTTG) targeting exon 16 of *RB1* gene were selected and cloned into pX335-U6-Chimeric_BB-CBh-hSpCas9n(D10A)(Puro^{R}), respectively to generate the guide plasmids. For electroporation, 10^7 cells were re-suspended with 0.6 ml Embryo Max Electroporation Buffer (Millipore), mixed with CRISPR/Cas9 nickase plasmids (25 μg each) and electroporated at 300 V/500 μF in a BIO-RAD Gene Pulser Xcell System. Following electroporation, cells were immediately dispensed into 10 cm MEF-coated plates in hESC medium (DMEM/F12 (Corning) with 20% KnockOut Serum replacement (Life Technologies), 1% Gibco GlutaMax (Life Technologies), 1% NEAA (Corning), 0.0007% β-mercaptoethanol (Sigma) and 10 ng/ml FGF2 (EMD Millipore)) supplemented with 10 μM ROCK inhibitor. After 48 h recovery, cells were treated with 1 μM puromycin (Sigma) for 48 h and then maintained in regular hESC medium for colony growth. The isolated genomic DNA from individual colonies was used for clonal identification by PCR using a *RB1* exon 16 specific primer set (forward: 5′-TCTGTTTCAGGAAGAAGAACGAT-3′; reverse: 5′-ACCATGGAGGTTACAGCAGTG-3′). The PCR fragments of wild-type and deletion of *RB1* exon 16 were examined by Sanger sequencing.

Quantitative real-time PCR

Total mRNA was isolated using TRIzol (Invitrogen) following the manufacturer's instructions. 1 μg of RNA was used for reverse transcription. Real-time PCR analysis was performed on a CFX96 machine (Bio-Rad) using the SYBR Green PCR Master Mix (Bio-Rad). The PCR reaction consisted of 10 μl SYBR Green PCR Master Mix, 1 μl of 10 μM forward and reverse primers, and 1 μl of 3-times diluted template cDNA in a total volume of 20 μl. Samples were analyzed in triplicate and normalized to GAPDH expression. The primer sequences are shown in Table 1.

In vitro differentiation

In vitro differentiation of H1-*RB1*(E16)$^{-/+}$ cells to HPCs, MSCs, and NPCs was performed by well-defined differentiation protocols described previously (Chambers et al., 2009; Qin et al., 2016; Zhao et al., 2015). For cell characterization, SOX17 (R&D Systems) and HNF4A (Cell Signaling Technology) were used for HPCs, CD105 (Thermo Fisher Scientific) and CD73 (BD Biosciences) were used for MSCs, and PAX6 (BioLegend) and NESTIN (BioLegend) were used for NPCs.

Table 1
Characterization and validation.

Classification	Test	Result	Data
Morphology	Photography	Normal	Fig. 1 panel D
Phenotype	Immunocytochemistry	NANOG, OCT4, SSEA4, TRA-1-81 and AP-positive.	Fig. 1 panel D
	RT-qPCR	Comparable of *NANOG*, *OCT4*, *SOX2*, *DPPA4*, and *REX1* expression with H1.	Fig. 1 panel E
Genotype	Karyotype (G-banding) and resolution	46 XY Resolution: 450–500	Fig. 1 panel H
Identity	Microsatellite PCR (mPCR) OR	N/A	N/A
	STR analysis	14/14 sites matched	Supplementary Table S1
Mutation analysis (IF APPLICABLE)	Sequencing	Heterozygous deletion of 50 bp in *RB1* exon 16.	Fig. 1 panel B
	Southern Blot OR WGS	N/A	N/A
Microbiology and virology	Mycoplasma	Mycoplasma test shows negative.	Fig. 1 panel G
Differentiation potential	Directed *in vitro* differentiation	Expression of SOX17 and HNF4A in HPCs, CD105 and CD166 in MSCs, and PAX6 and NESTIN in NPCs.	Fig. 1 panel I, J, and K
Donor screening (OPTIONAL)	HIV 1 + 2 Hepatitis B, Hepatitis C	N/A	N/A
Genotype additional info (OPTIONAL)	Blood group genotyping	N/A	N/A
	HLA tissue typing	N/A	N/A

Table 2
Reagents details.

Antibodies used for immunocytochemistry			
	Antibody	Dilution	Company Cat# and RRID
Pluripotency markers	Goat anti-NANOG	1:400	R and D Systems Cat# AF1997 RRID:AB_355097
Pluripotency markers	Rabbit anti-OCT4	1:250	Santa Cruz Biotechnology Cat# sc-9081 RRID:AB_2167703
Pluripotency markers	Mouse anti-SSEA4	1:200	R and D Systems FA1435P-025
Pluripotency markers	Mouse anti-TRA-1-85	1:400	R and D Systems Cat# FAB3195A RRID:AB_663789
Differentiation markers	Anti-CD105	1:400	Thermo Fisher Scientific Cat# 12-1057-42 RRID:AB_1311123
Differentiation markers	Anti-CD73	1:400	BD Biosciences Cat# 550257 RRID:AB_393561
Differentiation markers	Rabbit anti-HNF4a	1:1000	Cell Signaling Technology Cat# 3113S RRID:AB_2295208
Differentiation markers	Goat anti-SOX17	1:500	R and D Systems Cat# AF1924 RRID:AB_355060
Differentiation markers	Rabbit anti-PAX6	1:200	BioLegend Cat# 901301 RRID:AB_2565003
Differentiation markers	Mouse anti-NESTIN	1:200	BioLegend Cat# 655102 RRID:AB_2562023
RB1 (Western Blot)	Mouse anti-RB1	1:250	BD Biosciences Cat# 554136 RRID:AB_395259
Secondary antibodies	Goat anti-rabbit IgG(Alexa Fluor 488 conjugate)	1:1000	Jackson ImmunoResearch Labs Cat# 111-545-144 RRID:AB_2338052
Secondary antibodies	Donkey Anti-Goat IgG (Alexa Fluor488 conjugate)	1:1000	Jackson ImmunoResearch Labs Cat# 705-545-003 RRID:AB_2340428
Secondary antibodies	Donkey Anti-Mouse IgG (Alexa Fluor488 conjugate)	1:1000	Jackson ImmunoResearch Labs Cat# 715-545-150 RRID:AB_2340846
Secondary antibodies	Donkey Anti-Rabbit IgG (Cy3 conjugate)	1:1000	Jackson ImmunoResearch Labs Cat# 711-165-152 RRID:AB_2307443
Secondary antibodies	Donkey Anti-Rabbit IgG (Cy5 conjugate)	1:1000	Jackson ImmunoResearch Labs Cat# 711-175-152 RRID:AB_2340607

Primers		
	Target	Forward/reverse primer (5′–3′)
Pluripotency markers (qPCR)	OCT4	AACCTGGAGTTTGTGCCAGGGTTT/TGAACTTCACCTTCCCTCCAACCA
Pluripotency markers (qPCR)	SOX2	AGAAGAGGAGAGAGAAAGAAAGGGAGAGA/GAGAGAGGCAAACTGGAATCAGGATCAAA
Pluripotency markers (qPCR)	NANOG	TTTGTGGGCCTGAAGAAAACT/AGGGCTGTCCTGAATAAGCAG
Pluripotency markers (qPCR)	DPPA4	GACCTCCACAGAGAAGTCGAG/TGCCTTTTTCTTAGGGCAGAG
Pluripotency markers (qPCR)	REX1	GCCTTATGTGATGGCTATGTGT/ACCCCTTATGACGCATTCTATGT
House-keeping genes (qPCR)	GAPDH	CCACTCCTCCACCTTTGAC/ACCCTGTTGCTGTAGCCA
Targeted mutation analysis/sequencing	RB1 exon16	TTCTTTTTATAGAAGTAAGTATTTTATAATC/CTCAAAGGTCTTCGGAGGGA

Immunofluorescent staining and immunoblotting

H1-*RB1*(E16)$^{-/+}$cells or differentiated cells were fixed with 4% paraformaldehyde in PBS for 10 min at room temperature, blocked with 10% serum in 0.1% PBST for 1 h and incubated with the indicated primary antibodies (Table 2) overnight. Cells were then washed with PBST, incubated with corresponding secondary antibodies for 1 h at room temperature, and detected by Leica DMi8. Immunoblotting was performed as described (Lee et al., 2007).

Mycoplasma test

PCR mycoplasma test kit was used according to the manufacturer's instructions (abm G238).

Karyotype analysis and STR analysis

The G-banding karyotype was performed by The T. C. Hsu Molecular Cytogenetics Facility in The University of Texas M.D. Anderson Cancer Center. Twenty metaphase chromosome spreads were analyzed with G-band resolution of 450–500. STR analysis for parent cell authentication was performed by the Characterized Cell Line Core Facility in The University of Texas M.D. Anderson Cancer Center. 14 STR loci were compared using the Promega Powerplex 16 HS kit. Fragments were amplified by PCR for further analysis.

Supplementary data to this article can be found online at https://doi.org/10.1016/j.scr.2018.01.021.

Conflict of interest

The authors declare no conflict of interest.

Acknowledgements

We thank Dr. A.S. Multani for performing karyotype analysis and Dr. F. Zhang for CRISPR/Cas9 nickase plasmid. J.T. and Z.H. are supported by the Ke Lin Program of the First Affiliated Hospital of Sun Yat-sen University. D.H. is supported by State-sponsored Joint Ph.D. Program from China Scholarship Council (201606380093). R.Z. is supported by UTHealth Innovation for Cancer Prevention Research Training Program Pre-doctoral Fellowship (Cancer Prevention and Research Institute of Texas grant RP160015) and Wei Yu Family Endowed Scholarship (The University of Texas MD Anderson Cancer Center UTHealth Graduate School of Biomedical Sciences). D.-F.L. is the CPRIT scholar in Cancer Research and supported by NIH Pathway to Independence Award R00 CA181496 and CPRIT Award RR160019.

References

Chambers, S.M., Fasano, C.A., Papapetrou, E.P., Tomishima, M., Sadelain, M., Studer, L., 2009. Highly efficient neural conversion of human ES and iPS cells by dual inhibition of SMAD signaling. Nat. Biotechnol. 27:275–280. https://doi.org/10.1038/nbt.1529.

Lee, D.F., Kuo, H.P., Chen, C.T., Hsu, J.M., Chou, C.K., Wei, Y., Sun, H.L., Li, L.Y., Ping, B., Huang, W.C., He, X., Hung, J.Y., Lai, C.C., Ding, Q., Su, J.L., Yang, J.Y., Sahin, A.A., Hortobagyi, G.N., Tsai, F.J., Tsai, C.H., Hung, M.C., 2007. IKK β Suppression of TSC1 links inflammation and tumor angiogenesis via the mTOR pathway. Cell 130: 440–455. https://doi.org/10.1016/j.cell.2007.05.058.

Lin, Y.H., Jewell, B.E., Gingold, J., Lu, L., Zhao, R., Wang, L.L., Lee, D.F., 2017. Osteosarcoma: molecular pathogenesis and iPSC modeling. Trends Mol. Med. https://doi.org/10.1016/j.molmed.2017.06.004.

Qin, J., Chang, M., Wang, S., Liu, Z., Zhu, W., Wang, Y., Yan, F., Li, J., Zhang, B., Dou, G., Liu, J., Pei, X., Wang, Y., 2016. Connexin 32-mediated cell-cell communication is essential for hepatic differentiation from human embryonic stem cells. Sci. Rep. 6. https://doi.org/10.1038/srep37388.

Zhao, Q., Gregory, C.A., Lee, R.H., Reger, R.L., Qin, L., Hai, B., Park, M.S., Yoon, N., Clough, B., McNeill, E., Prockop, D.J., Liu, F., 2015. MSCs derived from iPSCs with a modified protocol are tumor-tropic but have much less potential to promote tumors than bone marrow MSCs. Proc. Natl. Acad. Sci. 112:530–535. https://doi.org/10.1073/pnas.1423008112.